RESEARCH PAPER

In-silico investigation of Antiviral Compounds Against Canine Parvovirus via Molecular Docking and Molecular Dynamics Studies

Stephen Ilango[1*], Sittarthan Viswanathan[1], Jayaraman Rajangam[1], Aravinth Velmurugan[2] Gowrishankar Jayabalan[3] & Pradeep S[4]

[1*]Department of Pharmacology, Shri Venkateshwara College of Pharmacy, Puducherry
[1]Department of Pharmacology, Shri Venkateshwara College of Pharmacy, Puducherry
[1]Department of Pharmacology, Shri Venkateshwara College of Pharmacy, Puducherry
[2]Department of Pharmacognosy, School of Pharmacy, Sri Balaji Vidyapeeth University, Puducherry
[3]Department of Pharmacognosy, School of Pharmacy, Sri Balaji Vidyapeeth University, Puducherry, Karaikal
[4]Department of Biotechnology, College of Engineering, B.M.S, Bengaluru, Karnataka

***Corresponding Author:** Stephen Ilango
Mail id: stephenillango5@gmail.com, **Website**: https://svcppondy.ac.in/ https://sbvu.ac.in/sop/

Abstract
Canine parvovirus (CPV-2) is one of the most important pathogens of dogs of all ages, causing pandemic infection that are characterized by fatal hemorrhagic enteritis. CPV-2 has high morbidity and mortality rates in canines. CPV-2 is self-replicating parvovirus that causes enteritis and myocarditis in dogs. CPV-2 is a highly contagious virus affecting dogs worldwide, posing a significant threat. SR9009 on CPV-2 remains unidentified, we have found that SR9009 has binding affinity to CPV-2 target. SR9009 is a specific synthetic agonist of the REV-ERBs, essential circadian clock components. SR9009 a synthetic pyrrole derivative that acts as REV- ERBs-specific agonist. Hence it interests to document analysis of SR9009 with CPV-2 target and also has good score binding affinity.
Keywords: Molecular modelling, Molecular Docking, Molecular Dynamics, SR9009 and CPV-2 target
How to cite this article: Ilango S, Viswanathan S, Rajangam J, Velmurugan A, Jayabalan G, Pradeep S. In-silico investigation of Antiviral Compounds Against Canine Parvovirus via Molecular Docking and Molecular Dynamics Studies. Int J Drug Deliv Technol. 2026;16(70s): 1137-1149. DOI: 10.25258/ijddt.16.70s.121

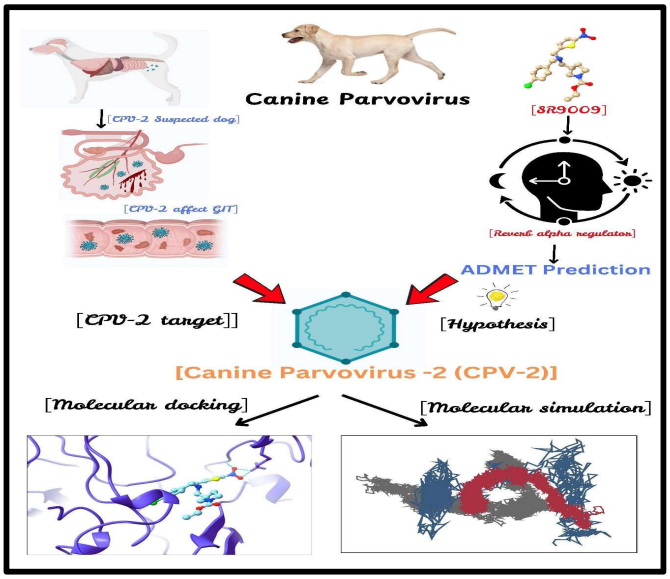

Figure 1: Graphical Abstract

*Author for Correspondence: stephenillango5@gmail.com

Introduction

Canine parvovirus 2 [CPV- 2], causative agent of acute hemorrhagic enteritis, myocarditis in dogs and one of the most important pathogenic viruses. Highly contagious and often fatal diseases. CPV- 2 was first recognized in 1977 and well established as an enteric pathogen of dogs throughout world with high morbidity 100 percent and frequent mortality up to 10 percent. CPV is believed to originated as host range variant from feline panleukopenia (FPV) [1]. Parvoviridae family consist of 2 subfamily *Parvovirinae* and *Densovirinae* infecting vertebrates and insects. Currently 5 genera are included in subfamily of *Parvovirinae* namely *Parvovirus*, *Erythrovirus, Dependovirus*, *Amdovirus* and *Bocavirus*. Canine parvovirus (CPV) belongs to the genus Parvovirus and has been included in unique species of feline panleukopenia virus (FPV) [2]. Canine parvovirus is the mostly recognized cause of transmissible viral diarrhoea in dogs and one of the most common infectious diseases of dogs in worldwide. It is caused by variants of the genus *Parvovirus*-2 [CPV-2], which are members of the genus *Parvovirus*. CPV-2 emerged in the early to mid-1970s and caused a worldwide pandemic of illness in dogs [3]. In 1980s CPV-2 evolved into two variants [CPV-2a and CPV-2b] and while in 2000, third variant [CPV- 2C] remained found in Italy and found in all continents except Australia. All 3 variants are believed to have similar pathogenicity leading to indistinguishable clinical disease [4]. CPV-2 evolved into 3 antigenic variants called CPV-2a in the United States, Japan, Denmark and Australia in 1980. CPV-2b in the United States in 1984 and CPV-2c in Italy in 2001. The virus was first reported in Egypt in 1982 when it was isolated from military dogs exhibiting the clinical signs of CPV-2 [5]. Recently, the incidence of CPV-2 infections associated with CPV- 2C genotypes has increased in several provinces of China [6]. First case of CPV-2 infection in India was document in 1982. Past 3-4 years there has been increased CPV-2 incidence and mortality in the dog population of the North East region (NER) of India based on personal consultation with physician. CPV-2 in the canine population in the entire NER, India revealed the occurrence of severe clinical disease that resulted in mortality towards affected dogs [7]. Incidence of parvovirus infection in dogs in the range of 6.93% to 65.04% [8]. SR9009 showed the highest antiviral activity and extensively studies *in vivo* [9].

SR9009 has shown promise in altering circadian regulation and exhibiting antiviral properties against influenza. The Rev-erb agonist SR9009 exhibits antiviral properties against influenza by altering circadian regulation [10]. SR9009 was successfully able to inhibit replication of alphavirus like chikungunya virus by suppressing the synthesis of the structural proteins [11].

Oseltamivir, an antiviral drug used primarily for the treatment of human influenza, is a neuraminidase inhibitor that has been studied in puppies with CPV enteritis and study confirmed that Oseltamivir treated animals decrease in morbidity and mortality Neuraminidase is an important enzyme used by pathogenic bacteria invading through the protective mucous barrier of the GI tract. The invasion through mucous barrier is biochemically similar to the budding virus from cell membrane, oseltamivir able to inhibit [12]. Oseltamivir has been shown to prevent weight loss and improve white blood cells in Canine Parvoviral Enteritis [CPE] with no major adverse effects; therefore, Oseltamivir may be an antiviral therapy for CPE [13].

In recent years, laboratory studies revealed broad-spectrum antiviral activity of nitazoxanide, rounding out a remarkably broad spectrum of activity for this drug and prompting efforts to develop nitazoxanide a new class of antiviral agents. Drug being repurposed as a new broad- spectrum agent with novel mechanism of action for treatment of influenza [14].

Nitazoxanide is a nitazoxanide benzamide derivative. Nitazoxanide also has antibacterial and antiviral activities it's found that nitazoxanide was able to inhibit CPV replication *in vitro* [15].

Considering the beneficial effects of REV-ERB alpha agonist like SR9009 which originally developed to study circadian rhythms can therefore implemented as a unique therapeutic drug against CPV-2 target.

We hypothesis that SR9009 a Reverb agonist has antiviral activity has been reported but not reported on canine parvovirus – 2 (CPV-2) target to attempt to validate clear mechanism of action SR9009 with CPV-2 target through *in-silico* approach.

Methodology

Molecular docking is a structure-based drug design method that stimulate the molecular interaction and predicts the binding mode and affinity between receptors and ligands [16]. *In silico* design which uses computational techniques in drug discovery process is being used to streamline. Accelerate hit identification and hit-to-lead optimization process [17]. Pre-docking steps ligand preparation, protein preparation and active site determination.

Hardware, software & Website

Hardware been used in laptop with Intel® Core i7-1255U RAM 16.0 GB @ 1.70 GHz, 64-bit operating system at windows 11.

Software for molecular docking analysis using MGL tools 1.5.7 were downloaded from (https://ccsb.scripps.edu/mgltools/downloads/) [18-Link]. To remove water molecular and particular chain of protein and converted pdb format using Pymol 2.5.4 were downloaded from (https://pymol.org/edu/) [19-Link]. Ligand and protein interaction visualized using Chimera X were downloaded from ((https://www.cgl.ucsf.edu/chimerax/download.html) [20-Link]. Molecular dynamics, Groningen machine for chemical simulation (Gromacs) software 2020.4 has been used. ADMET properties were done using pkCSM web tool

(https://biosig.lab.uq.edu.au/pkcsm/prediction) [21-Link]. Structural ligands were downloaded from Pubchem database (https://pubchem.ncbi.nlm.nih.gov/) [22-Link]. Protein was download from RCSB Protein Data Bank (PDB) (http://www.rcsb.org/pdb/) [23-Link]. Active site of proteins were selected from PDBsum (https://www.ebi.ac.uk/thornton srv/databases/pdbsum/) [24-Link] and Computed atlas of surface topology of proteins (CASTp) (http://sts.bioe.uic.edu/castp/index.html?2011) [25-Link]. For Toxicity assessment Protox-III open source Builder (ATB) web server (https://atb.uq.edu.au/) [27-Link].

ADME, physiochemical properties, drug likeness and toxicity prediction:

Comprehensive chemical compound data, which includes Simplified Molecular Input Line- Entry System (SMILES) data, was retrieved from Pubchem Database. Later, physicochemical and pharmacokinetic analyses were performed using the pkCSM web tool by inputting the SMILES code. After entering the SMILES code, users can choose to select "ADMET" option on the pkCSM platform and patiently wait for the analysis process to complete. This method provides valuable insights into the absorption, distribution, metabolism, excretion and toxicity (ADMET) Swiss ADME were used for screening of Physiochemical properties and drug- likeness properties and developed by Swiss Institute of Bioinformatics. Lipinski [28], Ghose [29], Veber [30], Egan [31] and Muegge [32] rules of 5 screening were used for determining Drug like properties. Abbot bioavailability score was used to determining the bioavailability of ligands. Structure SMILE code of ligands was submitted to servers and results were further analyzed.

Protein preparation:

Canine parvovirus target CPV-2 were downloaded from RCSB PDB database. X-Ray diffraction resolution size not more than of 3.0 Å of targeted protein were used [33]. Water molecules and hetero groups were removed from protease structure using Pymol.

Ligand preparation:

Structural information and structure of ligands were obtained from PubChem database were download in SDF format and converted into PDB format using Pymol for docking analysis. SR9009 (PubChem CID: 57394020), Oseltamivir (PubChem CID: 65028) and Nitazoxanide (PubChem CID: 41684) were chosen as ligand. Oseltamivir and Nitazoxanide were chosen as standard. SR9009 taken as test. To start with docking analysis before that conformation with Lipinski rule of 5 and Toxicity study results of test ligand (SR9009) [34].

Molecular docking:

For docking analysis Autodock tools 1.5.7 version software was used. Active site residue was identified by computed atlas of surface topography of protein server (CASTp) [35]. PDBsum have clefts section have highlights binding sites on the protein surface [36]. Common active site was selected from both websites. Protein and ligands of pdbqt files were prepared and grid box were created using AutoDock tools and then polar hydrogens, Kollman charges were added [37]. Set to 80 × 80 × 80 with grid spacing of 0.375 Å. Docking parameter file (dpf) and Grid parameter file (Gpf) were created to run autogrid and autodock application. Genetic Algorithm (GA), (https://tox.charite.de/) were made to get docking analysis report. Lowest binding docking score with hydrogen bonding usually considered as best ligan-protein complex analysed using Chimera X [38].

Molecular dynamics simulation analysis:

The Crystal Structure of the protein-inhibitor complex was considered for the dynamics. The selected ligand from docking analysis CPV-SR9009 and CPV-STD was taken. Ligand topology was selected from the antechambers pdb2gmx, a module of GROMACS [PMID: 34844519], was used to add hydrogens to the heavy atoms [PMID: 32567989]. Prepared systems were first vacuum minimized for 1500 steps using the steepest descent. Then the structures were solvated in a cubic periodic box with a simple point charge (SPCE) water model [PMID: 35566187]. The complex systems were subsequently maintained with an appropriate salt concentration of 0.15 M by adding suitable numbers of Na and Cl counter ions [PMID: 31514687]. The system preparation was referred to on the basis of a previously published paper [PMID: 31514687]. Each resultant structure from the NPT equilibration phase was subjected for final production run in NPT ensemble for 100 ns simulation time. Finally, the trajectory of the simulation was analyzed using various tools provided by the Gromacs software package, including the protein root mean square deviation (RMSD), root mean square fluctuation (RMSF), radius of gyration (RG), solvent accessible surface area (SASA), hydrogen bonding (H-Bond). Molecular Mechanics Poisson-Boltzmann surface area (MM- PBSA) approach was employed to understand the binding free energy CPV-SR9009 and CPV- STD of an inhibitor with protein over simulation time. A GROMACS utility g_mmpbsa was employed to estimate the binding free energy [39]. To obtain an accurate result, we computed CPV-SR9009 and CPV-STD for the last 50 ns with dt 1000 frames.

Results

Values of Physiochemical and Lipophilicity properties of the ligands shown in [**Table 1**] **molecular weight** of the SR9009, Oseltamivir and Nitazoxanide indicate that 437.94, 312.40 and 307.28 were less than 500. **Hydrogen bond** donor all value less than 5 and Hydrogen bond acceptor all values less than 10, for all ligands **rotatable bond** less than 10 and **Topological polar surface** area only Nitazoxanide shows **142.35** indicate greater than 140 which is violation to Lipinski rule of 5 but SR9009 and Oseltamivir indicates 106.84

and 90.65 which lower than 140, obeys the Lipinski rule of 5. **Lipophilicity** of SR9009, Oseltamivir and Nitazoxanide indicates that 3.45, 1.38 and 1.16 which all three value less than 5 which obey the Lipinski rule of 5.

Table 1: Physiochemical and Lipophilicity properties of the ligands

Properties	SR9009	Oseltamivir	Nitazoxanide
Physiochemical Properties			
Molecular Formula	C20H24ClN3O4S	C16H28N2O4	C12H9N3O5S
Molecular weight	437.94 g/mol	312.40 g/mol	307.28 g/mol
Hydrogen Bond Donor	0	2	1
Hydrogen Bond Acceptor	5	5	6
Rotatable Bond	10	9	6
Molar Refractivity	120.13	84.52	76.65
Water Solubility Log S [ESOL]	Moderately soluble	Very Soluble	Soluble
Topological Surface area [Å^2]	106.84	90.65	**142.35**
Drug Likeness [Lipinski's rule of 5]			
Lipinski	0	0	0
Ghose	0	0	0
Veber	0	0	**1**
Egan	0	0	**1**
Muegge	0	0	0
Bioavailability Score	0.55	0.55	0.55
Lipophilicity			
Ilogp	3.62	2.56	0.90
XLOGP3	4.41	1.10	2.04
WLOGP	4.11	1.29	2.04
MLOGP	2.44	0.63	0.31
SILICOS-IT Log P	2.66	1.33	0.49
Consensus Log P	3.45	1.38	1.16

Pharmacokinetic result shown in [Table 2] of Nitazoxanide and Oseltamivir was higher **CaCO2 permeability** compared to SR9009. Nitazoxanide and SR9009 indicate that **Intestinal absorption** was high but, Oseltamivir was lower value. **skin permeability** properties were higher in SR9009 compared to Oseltamivir and Nitazoxanide. Only SR9009 has **P-glycoprotein** substrate property.

According to Distribution parameters, SR9009 it has **higher Volume of Distribution** [VDSS] distribution in body compared to oseltamivir and Nitazoxanide, shows **Poor BBB permeability** for three ligands and SR9009 only has good **CNS penetrate property** has promising drug candidate by targeting Central Nervous System compared to Oseltamivir and Nitazoxanide.

When comes to metabolic parameters, crucial and primary enzyme in the liver cells is cytochrome P450, SR9009 shows **inhibitory effects** in CYP2C9, CYP2D6 and CYP3A4 enzymes and remain **substrate** for CYP3A4 enzymes. For Nitazoxanide shows inhibitory effects in CYP1A2, CYP2C19 and CYP3A4 enzymes.

Regarding Excretion parameter, SR9009 and Oseltamivir shows that **higher total clearance value** compared to Nitazoxanide. Only SR9009 categorized as substrate for **Renal organic cationic transporter 2** [OCT2].

At last Toxicity assessment predicts that SR9009, Nitazoxanide has toxicity towards **AMES** and **Hepatotoxicity**. SR9009 required -0.233 low dose for maximum tolerated dose for human compared to Oseltamivir and Nitazoxanide. No toxic effect to Tetrahymena pyriformis for all ligands.

Overall, drug likeness predicted that only Standard [Nitazoxanide] has violation compared to Test [SR9009] and Standard [Oseltamivir] and even though we have taken as standard for molecular docking analysis.

Quality of protein structure Canine parvovirus – 2 [CPV-2] predicted by Ramachandran plot verification

Using PROCHECK shown in [**Figure 2**] shows 100% quality of protein and G- Factors 0.13 which good value for molecular docking analysis.

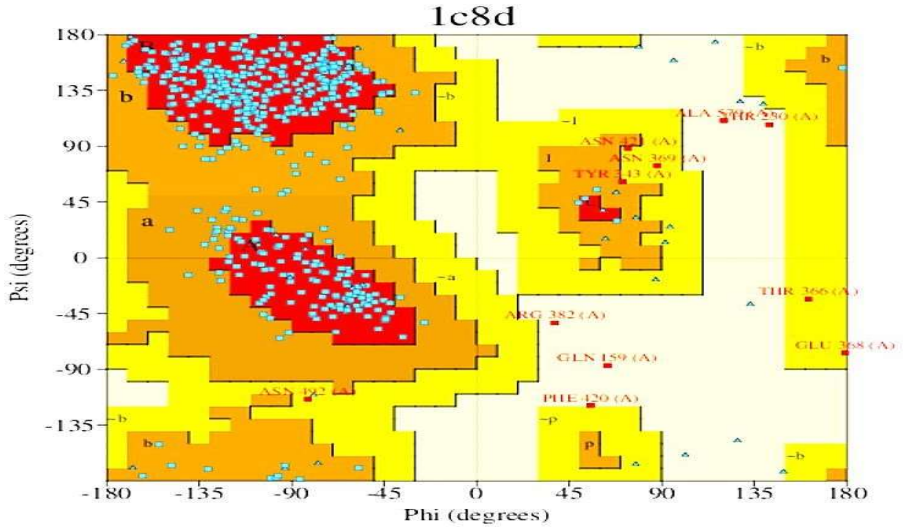

Figure 2: Canine parvovirus – 2 [CPV-2] predicted by Ramachandran plot verification Using PROCHEC

Table 2: Pharmacokinetic result of the ligands

PARAMETER	**SR9009**	**OSELTAMIVIR**	**Nitazoxanide**	**INDICATORS**
ABSORPTION				
Caco2 Permeability [**log Papp in 10^{-6} cm/s**]	0.473	0.934	1.215	High CaCO2 permeability value would be > 0.90
Intestinal Absorption [Human] [**% Absorbed**]	**86.336**	74.469	**87.975**	Poor absorption < 30%
Skin Permeability [**log Kp**]	-2.711	-3.177	-2.752	Low, log Kp > - 2.5
P-glycoprotein Substrate	Yes	No	No	Yes/No
DISTRIBUTION				
VDSS [Human] [**log L/kg**]	0.919	0.043	-0.786	Low, log < -0.15 High, log > 0.45
BBB permeability [**log BB**]	-0.358	-0.693	-0.959	Good, log BB > 0.3 Poor, log BB < -1
CNS permeability [**log PS**]	-2.212	-3.111	-2.678	Can penetrate, Log PS > -2 Cannot penetrate, Log PS < -3
METABOLISM				
CYP2D6 Substrates	No	No	No	Yes/No
CYP3A4 Substrates	**Yes**	No	No	Yes/No
CYP1A2 Inhibitors	No	No	**Yes**	Yes/No
CYP2C19 Inhibitors	No	No	**Yes**	Yes/No

CYP2C9 Inhibitors	**Yes**	No	No	Yes/No
CYP2D6 Inhibitors	**Yes**	No	No	Yes/No
CYP3A4 Inhibitors	**Yes**	No	**Yes**	Yes/No
EXCRETION				
Total Clearances	0.344	0.923	-0.04	Higher is better
Renal OCT2 Substrates	Yes	No	No	Yes/No
TOXICITY				
AMES Toxicity	Yes	No	Yes	Yes/No
Max. tolerated dose [Human] [**log mg/kg/day**]	-0.233	0.479	0.761	-
Hepatotoxicity	Yes	No	Yes	Yes/No
Skin Sensitization	No	No	No	Yes/No
T. Pyriformis toxicity [**log ug/L**]	0.374	0.106	0.409	Toxic, Log > 0.5 ug/L

Active site was determined by PDBsum and Castp online server common active site were selected [**Table 3**]. Molecular Docking analysis shows that among 3 ligands, Test [SR9009] shows higher affinity towards Canine parvovirus protein [CPV-2] **-8.04** kcal/mole compared to Standard Oseltamivir shows **-7.14** [kcal/mole] & Nitazoxanide shows **-7.18** kcal/mole. The CPV-2 which were docked with SR9009 visualized and interaction with Hydrogen bond residue Ile357, Ala379 and Lys354 shown in **[Figure 3]**

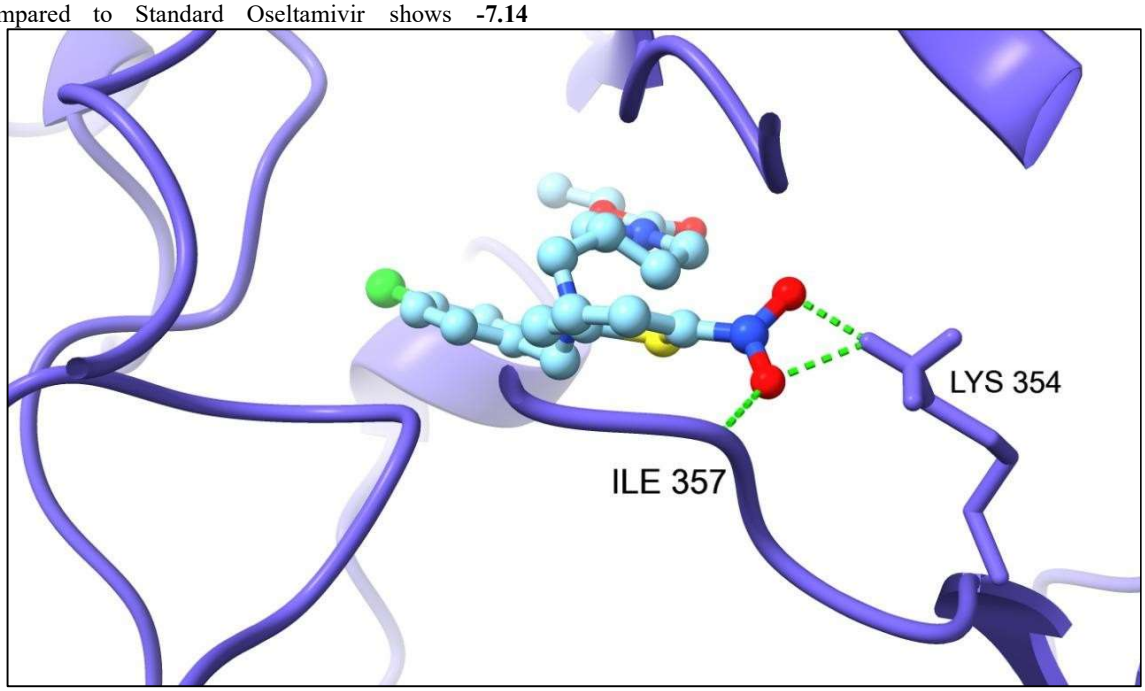

Figure 3: The CPV-2 which were docked with SR9009 visualized and interaction with Hydrogen bond residue Ile357, Ala379 and Lys354

After docking study, further expand to the MD simulation studies test [SR9009] and among 2 standard nitazoxanide has been selected for standard for simulation study based on the docking score. 100 ns simulation were used to assess the stability of both test [SR9009 + CPV-2] and Standard [Nitazoxanide + CPV-2] system.

Table 3: Active sites of 1C8D

PROTEIN	ORGANISM	PDB ID	ACTIVE SITE RESIDUE
Canine panleukopenia virus	Canine parvovirus	1C8D	Phe185, Pro187, Ala189, Met190, Tyr343, Lys354, Pro356, Ile357, Ala358, Ala359, Gln370, Arg377, Tyr378, Lys472, Phe474, Val484 and Asn485

3.1 Molecular Dynamics

The use of all-atom MD simulation is a suitable method for examining the structural dynamics of proteins and their interactions with ligands. This technique has revolutionized the field of computer-aided drug design and discovery, as it allows for a detailed analysis of molecular systems at the atomic level. In this study, MD simulations were performed to investigate the dynamic changes that occur upon binding of the target protein. Several parameters such as RMSD, RMSF, Rg, SASA and inter hydrogen bonding were calculated for both the protein and protein-ligand complex. CPV-STD represents Nitazoxanide throughout the study,

3.2 Root Mean Square Deviation (RMSD):

In order to investigate the stability of the protein-ligand complex and gain insight into the behavior of the systems, the RMSD values were analysed over time were shown in (**Figure 4**). The results indicate that both systems reached equilibrium within 20 ns and remained distributed evenly throughout the simulation. Moreover, the assessment of the RMSD values revealed that the CPV-SR9009 and CPV- Nitazoxanide maintained stability for up to 100 ns, indicating that the docked complex remained stable during the simulation. The average RMSD value for CPV-SR9009 and CPV-Nitazoxanide was determined to be 0.50 ± 0.07 nm and 0.68
± 0.12 nm. This finding suggests that CPV-SR9009 were stable but CPV- Nitazoxanide get fluctuated compared to test during the simulation.

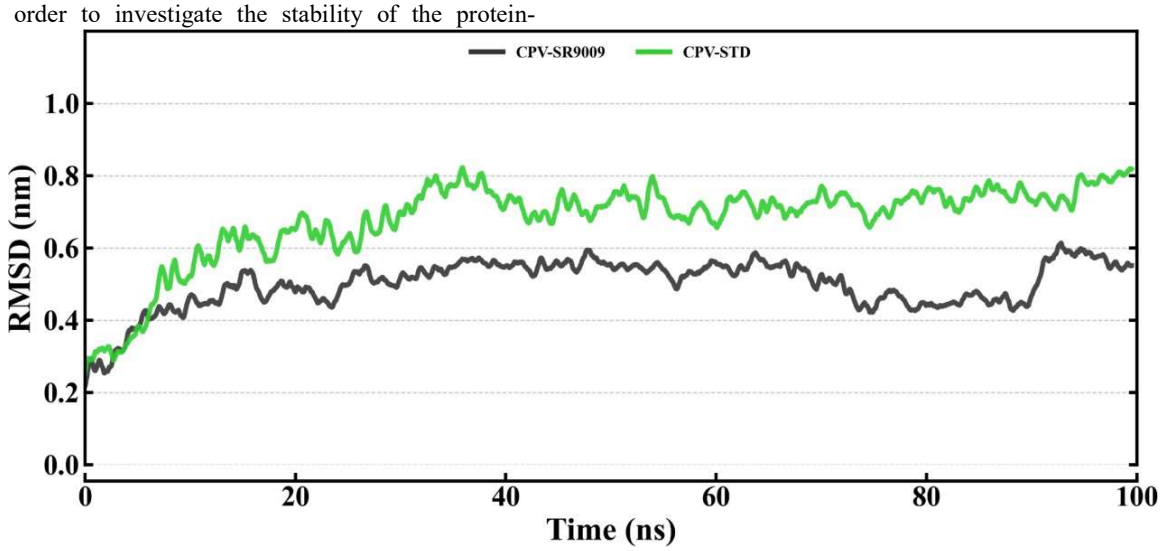

Figure 4: RMSD Conformational dynamics analysis of CPV-SR9009 and CPV-Nitazoxanide

3.3 Root Mean Square Fluctuation (RMSF)

To measure the fluctuations of each residue and flexible region in a protein during MD simulations, RMSF were assessed. By studying RMSF during simulations, the impact of ligand binding on the protein can be determined. Generally, compact protein structures such as sheets and helices have lower RMSFs, while loosely ordered loop regions have higher RMSF values. In this study, the RMSF values for each complex were calculated and plotted for every residue in the CPV-SR9009 and CPV- Nitazoxanide complexes were shown in [**Figure 5**]. The average RMSF value for CPV-SR9009 and CPV- Nitazoxanide was determined to be 0.18 ± 0.15 nm and 0.23 ± 0.18 nm. The results indicate that the CPV-SR9009 and CPV- Nitazoxanide complex did not significantly alter the overall RMSF distribution
.

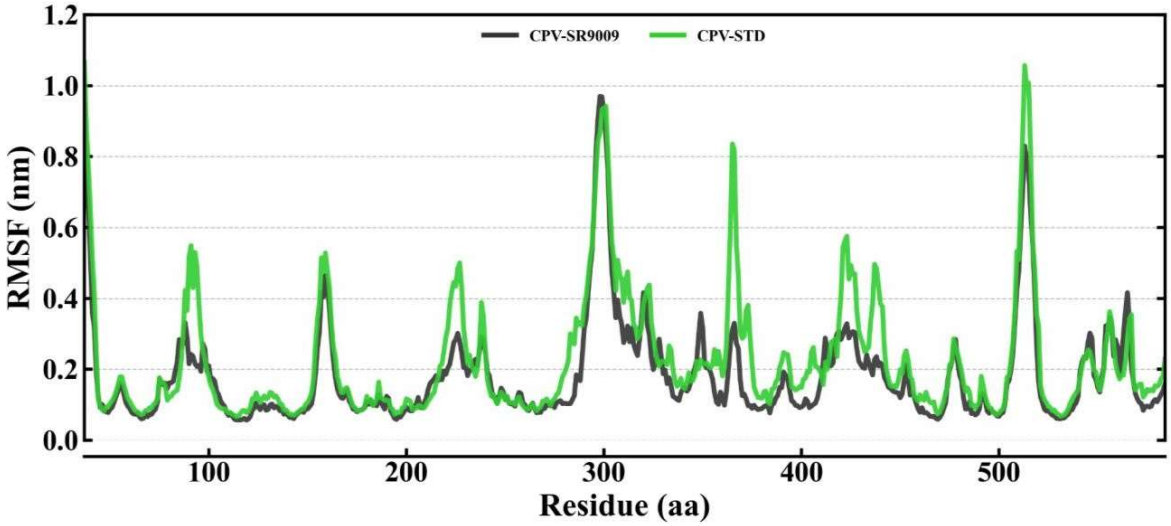

Figure 5: RMSF Conformational dynamics analysis of CPV-SR9009 and CPV- Nitazoxanide

3.4 Radius of gyration (Rg)

To assess the dynamic stability and compactness of the CPV-SR9009 and CPV- Nitazoxanide complex, the Rg value was computed and graphed over time were shown **[Figure 6]**. The average Rg value for CPV-SR9009 and CPV-Nitazoxanide was determined to be 2.79 ± 0.03 nm and 2.89 ± 0.02 nm.

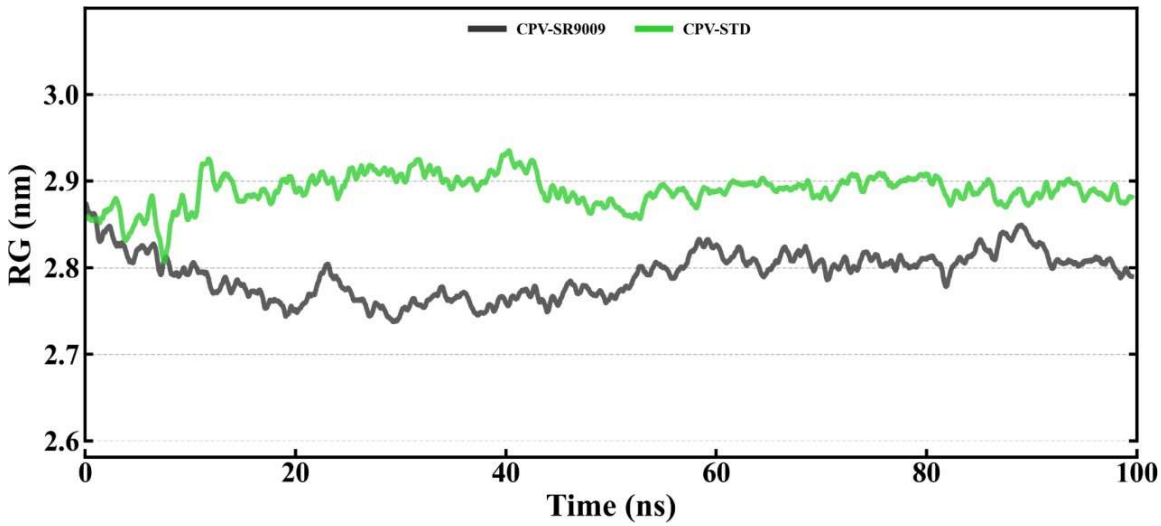

Figure 6: Rg Conformational dynamics analysis of CPV-SR9009 and CPV-Nitazoxanide complex.

3.5 Solvent accessible surface area (SASA)

To evaluate the accessibility of a protein molecule in a solvent environment, SASA is a useful parameter. In this study, the SASA values were calculated and plotted to determine the impact of CPV-SR9009 and CPV-STD binding on the solvent accessibility of the target was shown in **[Figure 7]**. The plot reveals a similar pattern in the SASA values of CPV-SR9009 and CPV- Nitazoxanide. The average SASA value for CPV-SR9009 and CPV- Nitazoxanide was determined to be 298.14 ± 6.76 nm and 304.33 ± 9.07 nm. The SASA values show fair equilibration without significant fluctuations throughout the simulation.

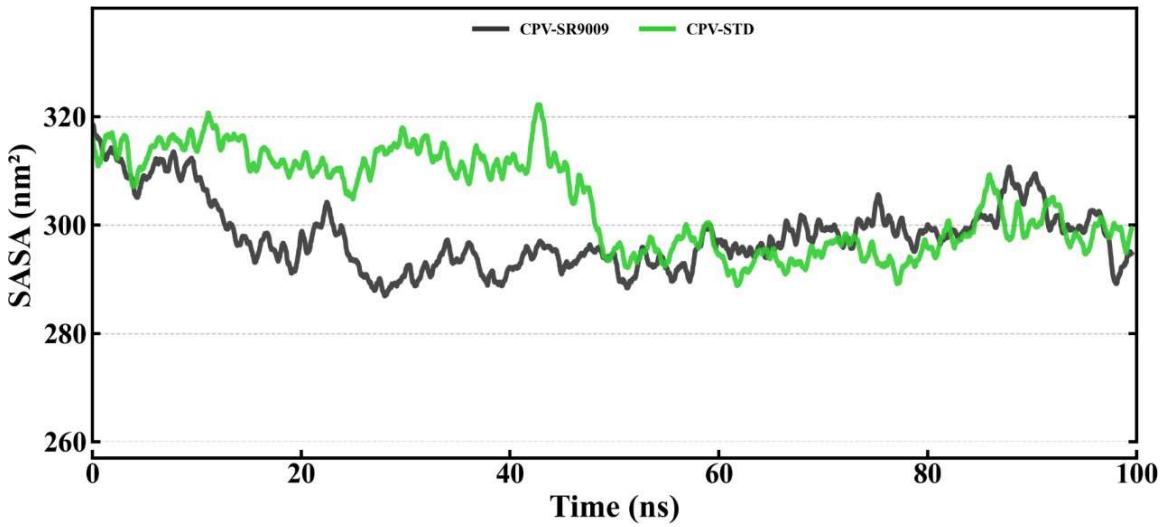

Figure 7: SASA Conformational dynamics analysis of CPV-SR9009 and CPV- Nitazoxanide complex

3.6 Intra and Inter Hydrogen Bond

To assess the stability of Protein alone (CPV-SR9009 and CPV-STD) interactions, the formation of Intra and Inter Hydrogen Bond plays a crucial role. In this study, we investigated the time-dependent behavior of Intra hydrogen bonds CPV-SR9009 and CPV- Nitazoxanide complexes and plotted the results were shown in **[Figure 8]**. The average Intra H-Bond value for Complex was determined to be 329.96 ± 9.36 nm and 327.08 ± 11.30 nm.

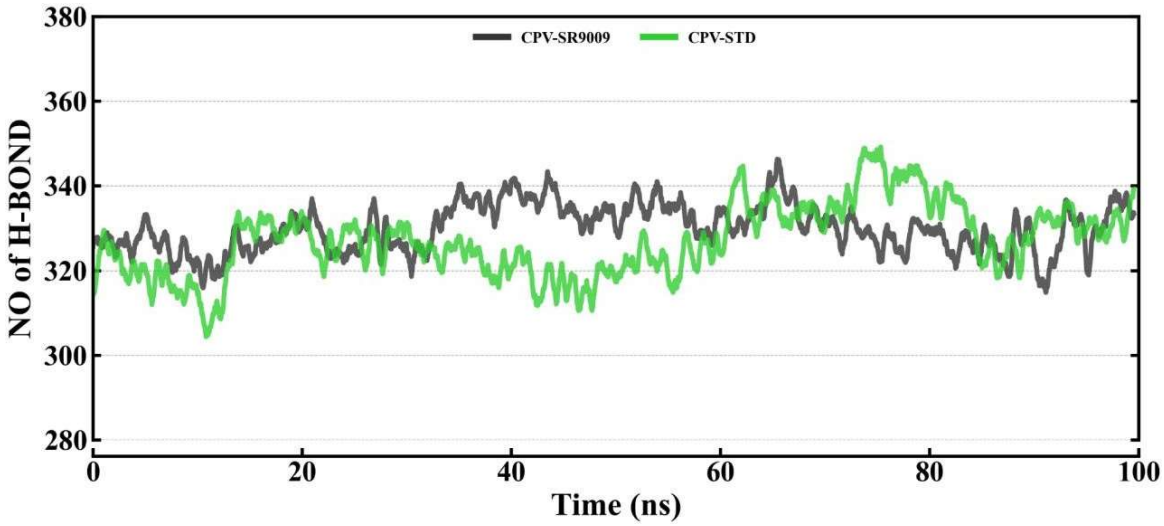

Figure 8: A] Intramolecular hydrogen bonds of CPV-SR9009 and CPV- Nitazoxanide during the simulation time.

To assess the stability of protein-ligand interactions, the formation of hydrogen bonds plays a crucial role. In this study, we investigated the time-dependent behavior of hydrogen bonds between CPV-SR9009 and CPV-STD and plotted the results. Our analysis indicates that the docked complex remained stable during the simulation, maintained by at least 0 to 6 hydrogen bonds with the CPV-SR9009 and CPV- Nitazoxanide.

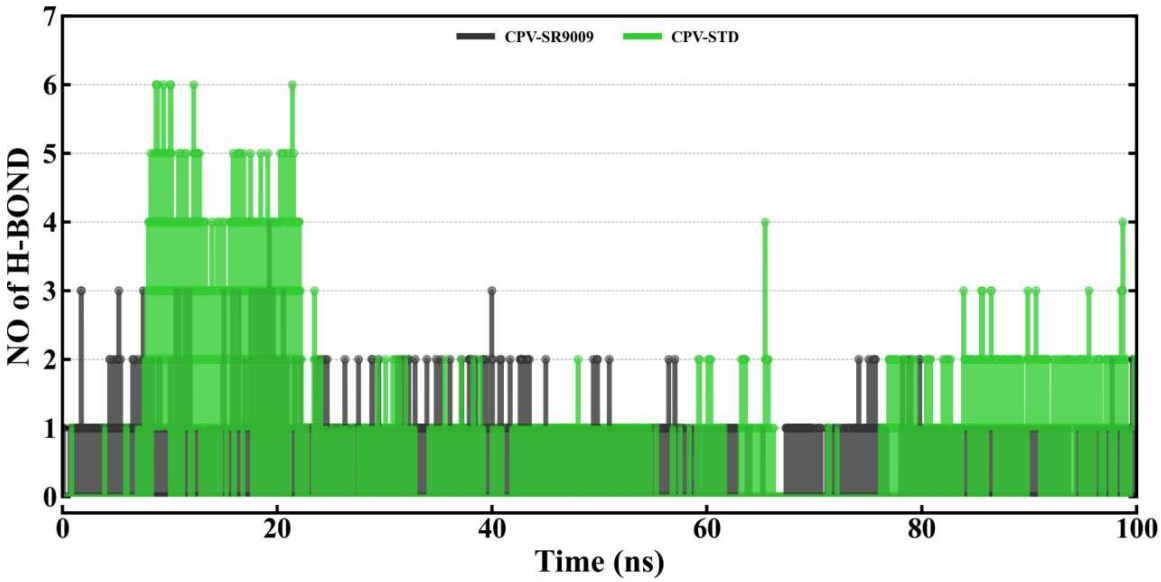

Figure 8: B] Intermolecular hydrogen bonds between protein-ligand during the simulation time.

3.7 Principal Component Analysis (PCA)

To explore the collective movements in CPV-SR9009 and CPV-STD we conducted PCA. The initial few eigenvectors (EVs) play a crucial role in the global motion of a protein molecule. Hence, we carried out PCA to study the conformational dynamics of CPV-SR9009 and CPV-STD during the simulation were shown in **[Figure 9]**. The time evolution of PCA dynamics, thus supporting the stability of the complex.

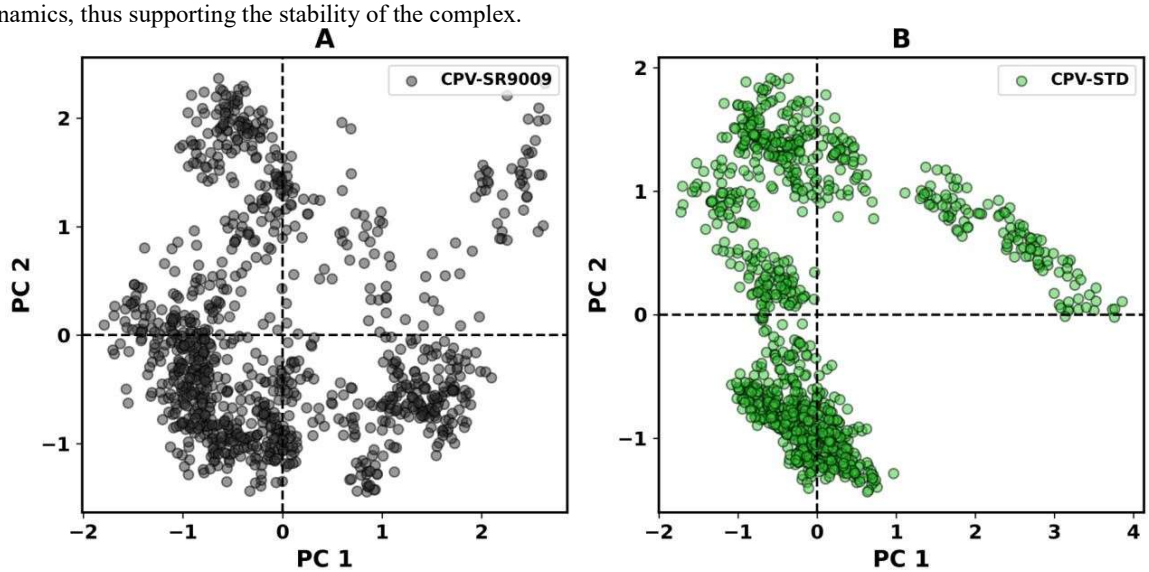

Figure 9: Principal component analysis 2D projection plot shows the conformation sampling of CPV-SR9009 and CPV- *Nitazoxanide* on PC1 and PC2.

3.8 Free Energy Landscapes (FELs):

The analysis of free energy landscapes (FELs) is a common approach to investigate protein folding mechanisms and overall stability. FEL plots provide a representation of the most stable conformational ensembles for a protein structure. Here, we generated FEL plots for PC1 and PC2 were shown in **[Figure 10]**, where deeper blue regions indicate a more stable suggests that the overall flexibility of the CPV-SR9009 and CPV-STD complex was reduced on both EVs, implying stability (Fig. XX). The plot clearly demonstrates that the CPV-SR9009 and CPV-STD complex occupied almost all the conformational motions and overlapped. In general, the lower number of movements observed in the CPV-SR9009 and CPV-STD suggests that CPV-SR9009 and CPV-STD did not significantly affect the target conformation and protein conformation with lower energy. The plots indicate energy values ranging 0 to 16 kJ/mol throughout the simulation of CPV-SR9009 and CPV-Nitazoxanide. The FEL plots reveal that the CPV-SR9009 and CPV-Nitazoxanide complex displays a single global minimum, confined to a large local basin. These findings suggest that CPV-SR9009 and CPV-Nitazoxanide do not cause any significant

conformational changes in the target structure, thus stabilizing it.

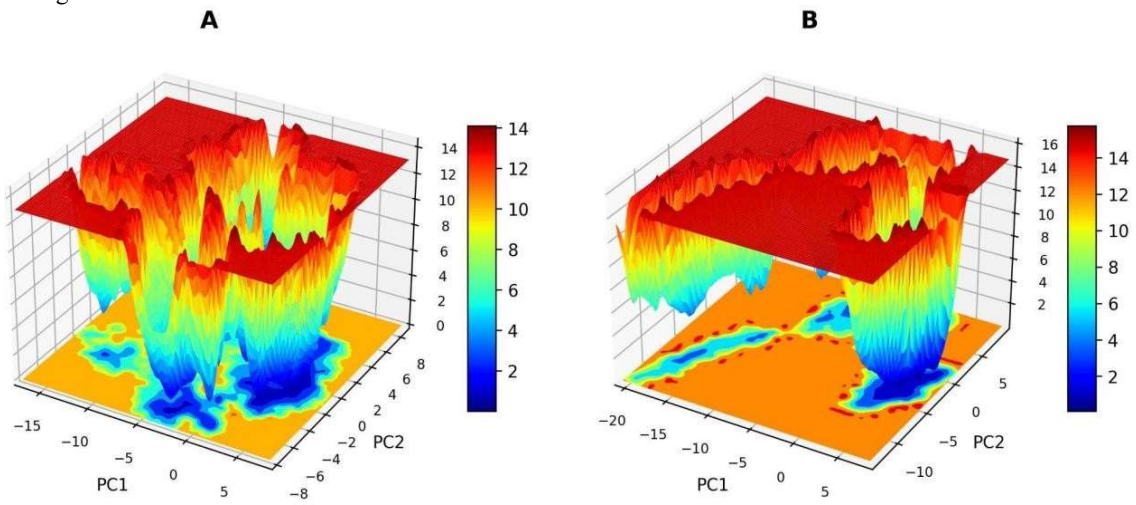

Figure 10: The free energy landscape plots for (A) CPV-SR9009, (B) CPV- Nitazoxanide

3.9 MM - PBSA

In order to determine the binding affinity of CPV-SR9009 and CPV-STD we examined the relative binding strength within the protein of summary energy. [Table 4] compares the binding strength of CPV-SR9009 and CPV-STD concerning inhibitors computed via the MM- PBSA method. Across a stable simulation trajectory, we calculate residue-level contributions to the interaction energy.

Table 4: comparison of binding strength of CPV-SR9009 and CPV-STD concerning inhibitors computed via the MM-PBSA method.

System	Van der Waal energy	Electrostatic energy	Polar solvation energy	SASA Energy	Binding energy
CPV- SR9009	-195.868 +/- 12.852 kJ/mol	-32.413 +/- 12.951 kJ/mol	127.642 +/- 20.056 kJ/mol	-18.960 +/- 1.141 kJ/mol	-119.598 +/- 11.808 kJ/mol
CPV-STD	-102.500 +/- 24.339 kJ/mol	-21.788 +/- 5.931 kJ/mol	88.293 +/- 26.117 kJ/mol	-11.333 +/- 2.159 kJ/mol	-47.328 +/- 4.363 kJ/mol

Discussion

Values of Physiochemical and Lipophilicity properties of the ligands molecular weight of the SR9009, Oseltamivir and Nitazoxanide indicate that 437.94, 312.40 and
307.28 were less than 500. Lipophilicity of SR9009, Oseltamivir and Nitazoxanide indicates that 3.45, 1.38 and 1.16 which all three value less than 5 which obey the Lipinski rule of 5. Nitazoxanide and SR9009 indicate that Intestinal absorption was high but, Oseltamivir was lower value. skin permeability properties were higher in SR9009 compared to Oseltamivir and Nitazoxanide. When comes to metabolic parameters,

crucial and primary enzyme in the liver cells is cytochrome P450, SR9009 shows inhibitory effects in CYP2C9, CYP2D6 and CYP3A4 enzymes and remain substrate for CYP3A4 enzymes. For Nitazoxanide shows inhibitory effects in CYP1A2, CYP2C19 and

CYP3A4 enzymes. Regarding Excretion parameter, SR9009 and Oseltamivir shows that higher total clearance value compared to Nitazoxanide. Only SR9009 categorized as substrate for Renal organic cationic transporter 2 [OCT2]. At last Toxicity assessment predicts that SR9009, Nitazoxanide has toxicity towards AMES and Hepatotoxicity. Overall, drug likeness predicted that only Standard [Nitazoxanide] has violation compared to Test [SR9009] and Standard [Oseltamivir] and even though we have taken as standard for molecular docking analysis. Quality of protein structure Canine parvovirus – 2 [CPV-2] predicted by Ramachandran plot verification Using PROCHECK shown in [Figure

1] shows 100% quality of protein and G-Factors 0.13 which good value for molecular docking analysis. Max. tolerated dose [Human]. T. Pyriformis toxicity [log ug/L] 0.374 0.106 0.409 Toxic, Log > 0.5 ug/L.

Molecular Docking analysis shows that among 3 ligands, Test [SR9009] shows higher affinity towards Canine parvovirus protein [CPV-2] -8.04 kcal/mole compared to Standard Oseltamivir shows -7.14 [kcal/mole] & Nitazoxanide shows -7.18 kcal/mole. The CPV-2 which were docked with SR9009 visualized and interaction with Hydrogen bond residue Ile357, Ala379 and Lys354 shown in [Figure 2].

After docking study, further expand to the MD simulation studies test [SR9009] and among 2 standard nitazoxanide has been selected for standard for simulation study based on the docking score. 100 ns simulation were used to assess the stability of both test [SR9009 + CPV-2] and Standard [Nitazoxanide + CPV-2] system. The use of all-atom MD simulation is a suitable method for examining the structural dynamics of proteins and their interactions with ligands.

In this study, MD simulations were performed to investigate the dynamic changes that occur upon binding of the target protein. In order to investigate the stability of the protein-ligand complex and gain insight into the behavior of the systems, the RMSD values were analyzed over time (Figure 3). The results indicate that both systems reached equilibrium within 20 ns and remained distributed evenly throughout the simulation. To measure the fluctuations of each residue and flexible region in a protein during MD simulations, RMSF is used. By studying RMSF during simulations, the impact of ligand binding on the protein can be determined. To assess the dynamic stability and compactness of the CPV-SR9009 and CPV-STD complex, the Rg value was computed and graphed over time (Figure 5). The average Rg value for CPV-SR9009 and CPV-STD was determined to be 2.79 ± 0.03 nm and 2.89 ± 0.02 nm. The plot reveals a similar pattern in the SASA values of CPV- SR9009 and CPV-STD. The SASA values show fair equilibration without significant fluctuations throughout the simulation. In this study, we investigated the time-dependent behavior of Intra hydrogen bonds CPV-SR9009 and CPV-STD complexes and plotted the results (Figure 7). The average Intra H-Bond value for Complex was determined to be 329.96 ± 9.36 nm and 327.08 ± 11.30 nm. To assess the stability of protein-ligand interactions, the formation of hydrogen bonds plays a crucial role. To explore the collective movements in CPV-SR9009 and CPV-STD we conducted PCA. FEL plots provide a representation of the most stable conformational ensembles for a protein structure. XX), where deeper blue regions indicate a more stable protein conformation with lower energy. Table XX compares the binding strength of CPV-SR9009 and CPV-STD concerning inhibitors computed via the MM-PBSA method. Across a stable simulation trajectory, we calculate residue-level contributions to the interaction energy.

Conclusion

Molecular docking and molecular dynamics predicted that SR9009 have higher binding affinity towards Canine parvovirus protein [CPV-2] target and it supported the further validation & Investigation in In-vitro and In-vivo methods for future perspectives.

REFERENCES

1. Nandi S, Kumar M. Canine parvovirus: current perspective. Indian J Virol. 2010 June;21(1):31–44.
2. Decaro N, Buonavoglia C. Canine parvovirus--a review of epidemiological and diagnostic aspects, with emphasis on type 2c. Vet Microbiol. 2012 Feb 24;155(1):1–12.
3. Sykes JE. Canine Parvovirus Infections and Other Viral Enteritides. Canine and Feline Infectious Diseases. 2014;141–51.
4. Mylonakis ME, Kalli I, Rallis TS. Canine parvoviral enteritis: an update on the clinical diagnosis, treatment, and prevention. Vet Med (Auckl). 2016 July 11; 7:91–100.
5. Ammar EF, Hegazy YM, Al-Gaabary M, Mosad SM, Salem M, Marzok M, et al. Epidemiological, and molecular investigation of Canine parvovirus-2 infection in Egypt. J Vet Sci. 2024 July;25(4):e56.
6. Umar S, Gao D, Kim S, Cheng Y, Fang Z, Zhongqi Q, et al. Molecular characterization of canine parvovirus type 2 (CPV2) reveals a high prevalence of the CPV2c genotype among dogs suffering from diarrhea. Animal Diseases. 2024 Jan 2;4(1):1.
7. Jayappa K, Rajkhowa TK, Gaikwad SS. Canine parvovirus in North-East India: a phylogenetic and evolutionary analysis. Vet Q. 2024 Dec;44(1):1–13.
8. Current Topics in Canine and Feline Infectious Diseases, An Issue of Veterinary Clinics: Small Animal Practice [Internet]. 2010 [cited 2025 Dec 31]. Available from: https://shop.elsevier.com/books/current-topics-in-canine-and-feline-infectious-diseases-an- issue-of-veterinary-clinics-small-animal-practice/barr/978-1-4377-2508-7
9. Zhuang X, Magri A, Hill M, Lai AG, Kumar A, Rambhatla SB, et al. The circadian clock components BMAL1 and REV-ERBα regulate flavivirus replication. Nat Commun. 2019 Jan 22;10(1):377.
10. Tseng YY. A theoretical systems chronopharmacology approach for COVID-19: Modeling circadian regulation of lung infection and potential precision therapies. CPT Pharmacometrics Syst Pharmacol. 2025 Feb;14(2):340–50.
11. Giri A, Srinivasan A, Sundar IK. COVID-19: Sleep, Circadian Rhythms and Immunity - Repurposing Drugs and Chronotherapeutics for SARS-CoV-2. Front Neurosci. 2021; 15:674204.
12. Mazzaferro EM. Update on Canine Parvoviral Enteritis. Vet Clin North Am Small Anim Pract. 2020 Nov;50(6):1307–25.
13. Ulas N, Ozkanlar Y, Ozkanlar S, Timurkan MO, Aydin H. Clinical and inflammatory response to antiviral treatments in dogs with parvoviral

enteritis. J Vet Sci. 2024 Jan;25(1): e11.
14. Rossignol JF. Nitazoxanide: a first-in-class broad-spectrum antiviral agent. Antiviral Res. 2014 Oct; 110:94–103.
15. Su X, Zhou H, Han Z, Xu F, Xiao B, Zhang J, et al. Transcriptional Differential Analysis of Nitazoxanide-Mediated Anticanine Parvovirus Effect in F81 Cells. Viruses. 2024 Feb 12;16(2):282.
16. Fan J, Fu A, Zhang L. Progress in molecular docking. Quant Biol. 2019 June 1;7(2):83–9.
17. Makhouri FR, Ghasemi JB. In Silico Studies in Drug Research Against Neurodegenerative Diseases. Curr Neuropharmacol. 2018;16(6):664–725.
18. mgl-admin. Downloads [Internet]. mgltools. [cited 2025 Dec 31]. Available from: https://ccsb.scripps.edu/mgltools/downloads/
19. Registration For Educational-Use Only PyMOL Builds [Internet]. [cited 2025 Dec 31]. Available from: https://pymol.org/edu/
20. Download UCSF ChimeraX [Internet]. [cited 2025 Dec 31]. Available from: https://www.cgl.ucsf.edu/chimerax/download.html
21. pkCSM [Internet]. [cited 2025 Dec 31]. Available from: https://biosig.lab.uq.edu.au/pkcsm/prediction
22. PubChem. PubChem [Internet]. [cited 2025 Dec 31]. Available from: https://pubchem.ncbi.nlm.nih.gov/
23. Bank RPD. RCSB PDB [Internet]. [cited 2025 Dec 31]. Available from: https://www.rcsb.org/pdb/
24. PDBsum1 home page [Internet]. [cited 2025 Dec 31]. Available from: https://www.ebi.ac.uk/thornton-srv/software/PDBsum1/
25. Tian W, Chen C, Lei X, Zhao J, Liang J. CASTp 3.0: computed atlas of surface topography of proteins. Nucleic Acids Research. 2018 July 2;46(W1): W363–7.
26. ProTox-3.0 - Prediction of TOXicity of chemicals [Internet]. [cited 2025 Dec 31]. Available from: https://tox.charite.de/protox3/index.php?site=compound_input
27. Malde AK, Zuo L, Breeze M, Stroet M, Poger D, Nair PC, et al. An Automated Force Field Topology Builder (ATB) and Repository: Version 1.0. J Chem Theory Comput. 2011 Dec 13;7(12):4026–37.
28. Lipinski CA, Lombardo F, Dominy BW, Feeney PJ. Experimental and computational approaches to estimate solubility and permeability in drug discovery and development settings. Adv Drug Deliv Rev. 2001 Mar 1;46(1–3):3–26.
29. Ghose AK, Viswanadhan VN, Wendoloski JJ. A knowledge-based approach in designing combinatorial or medicinal chemistry libraries for drug discovery. 1. A qualitative and quantitative characterization of known drug databases. J Comb Chem. 1999 Jan;1(1):55–68.
30. Veber DF, Johnson SR, Cheng HY, Smith BR, Ward KW, Kopple KD. Molecular properties that influence the oral bioavailability of drug candidates. J Med Chem. 2002 June 6;45(12):2615–23.
31. Egan WJ, Merz KM, Baldwin JJ. Prediction of drug absorption using multivariate statistics. J Med Chem. 2000 Oct 19;43(21):3867–77.
32. Muegge I, Heald SL, Brittelli D. Simple selection criteria for drug-like chemical matter. J Med Chem. 2001 June 7;44(12):1841–6.
33. Whey-Derived Peptides Interactions with ACE by Molecular Docking as a Potential Predictive Tool of Natural ACE Inhibitors - PubMed [Internet]. [cited 2026 Jan 2]. Available from: https://pubmed.ncbi.nlm.nih.gov/32013233/
34. Chandran SCS, Christopher I, Sounderraajan A, Murugesan V, Sabapathy I, Periyasamy V, et al. Molecular docking analysis of quercetin with known CoVid-19 targets. Bioinformation. 2023;19(11):1081–5.
35. Adi PJ, Yellapu NK, Matcha B. Modeling, molecular docking, probing catalytic binding mode of acetyl-CoA malate synthase G in Brucella melitensis 16M. Biochem Biophys Rep. 2016 Dec;8:192–9.
36. Carpenter KA, Altman RB. Databases of ligand-binding pockets and protein-ligand interactions. Comput Struct Biotechnol J. 2024 Dec; 23:1320–38.
37. Azam SS, Abbasi SW. Molecular docking studies for the identification of novel melatoninergic inhibitors for acetylserotonin-O-methyltransferase using different docking routines. Theor Biol Med Model. 2013 Oct 24; 10:63.
38. Vardhan S, Sahoo SK. Computational studies on searching potential phytochemicals against DNA polymerase activity of the monkeypox virus. J Tradit Complement Med. 2023 May 8;13(5):465–78.
39. Kumari R, Kumar R, Open-Source Drug Discovery Consortium, Lynn A. g_mmpbsa--a GROMACS tool for high-throughput MM-PBSA calculations. J Chem Inf Model. 2014 July 28;54(7):1951–62.